Mechanical Technology and Engineering Insights

www.mtei.reapress.com

Mech. Technol. Eng. Insights . Vol. 2, No. 2 (2025) 121–137.

Paper Type: Original Article

Forced Convection and MHD Effect of Non-Newtonian Fluids Along a Pipe

Mehdi Moslemi*

Department of Mechanical Engineering Ayandegan Institute of Higher Education, Tonekabon, Iran; mehdimoslemi1982@gmail.com.

Citation:

Received: 12 January 2025 *Revised: 14 March 2025* *Accepted: 26 April 2025*	Moslemi, M. (2025). Forced convection and MHD effect of non-Newtonian fluids along a pipe. *Mechanical Technology and Engineering Insights, 2*(2), 121-137.

Abstract

In this paper, the forced convection heat transfer of incompressible, Power law Non-Newtonian fluids through two-dimensional circular pipes in the presence of an external uniform magnetic field was considered. Moreover, momentum and energy equations are solved using a finite volume method and a simple algorithm. Two cases of the thermal boundary condition, a constant temperature and a constant heat flux at the wall, are investigated. The viscous and Joule dissipations are taken into account in the energy equation. Moreover, the influence of the magnetic field and flow behavior index (n) on the velocity distribution, the friction factor, and the Nusselt numbers is discussed. Also, the influence of the viscous and Joule dissipations on the Nusselt numbers is investigated. The results show that the magnetic field has a damping effect on the flow for all values of n. By increasing n, the maximum fluid velocity and friction factor will increase. Increasing n increases maximum fluid velocity and friction factor. Increasing the Hartmann number decreases maximum fluid velocity and increases the friction factor. Also, the increment in the Brinkman number decreases the value of the Nusselt number for all Hartmann numbers and n.

Keywords: Magnetohydrodynamic flow, Forced convection, Power-law fluid, Simple algorithm.

1 | Introduction

The study of Magnetohydrodynamic (MHD) viscous flows is important for industrial, technological, and geothermal applications, such as high-temperature plasmas, cooling of nuclear reactors, MHD accelerators, and power generation systems. On the other hand, several industrially important fluids, such as polymer solutions and melts, rubber, blood, molten plastics, polymers, pulps, and foods, exhibit Non-Newtonian fluid behavior. Due to the growing use of these non-Newtonian materials in various manufacturing and processing industries, considerable efforts have been made towards understanding their flow characteristics. Min et al. [1] studied analytically the fully developed laminar flow of a Bingham plastic in a circular pipe. Hossain [2]

Corresponding Author: mehdimoslemi1982@gmail.com

https://doi.org/10.48313/mtei.v2i2.44

determined that viscous and Joule heating effects on MHD free convection flows with variable plate temperature vary linearly with a distance from the leading edge in the presence of a uniform transverse magnetic field. The equations governing the flow were solved numerically by applying the finite difference method along with Newton's linearization approximation. Jha [3] studied the natural convection in unsteady Couette motion.

The problem of MHD flow and heat transfer with variable viscosity for Newtonian fluids in a rectangular duct with the Hall Effect has been investigated numerically by Sayed-Ahmed and Attia [4]. Sayed-Ahmed and Attia [5] investigated the effect of Hall current on MHD flow and heat transfer for Bingham fluids in a rectangular duct. Attia [6] investigated the Hall Effect on the Flow of a Dusty Bingham Fluid in a Circular Pipe. The problem of Numerical solution of power law fluid flow and heat transfer with a magnetic field in a rectangular duct and with velocity gradient dependent viscosity has been investigated numerically by Sayed-Ahmed [7].

It is of interest in this paper to study the influence of the magnetic field as well as the Non-Newtonian fluid characteristics on the friction factor and Nusselt number. The research has investigated the steady MHD laminar flow and heat transfer of viscous and incompressible electrically conducting Power law fluids through a 2D circular duct, where the fluid is subjected to an external uniform magnetic field. The momentum and energy equations, including the viscous and Joule dissipation terms, have been solved numerically using the finite volume method. The energy equation has been solved for a constant temperature and a constant flux at the wall. The influences of the magnetic field and the characteristics of the Non-Newtonian fluid on the velocity and temperature distributions have been studied.

2 | Mathematical Model

A steady laminar and axisymmetric horizontal flow of a viscous incompressible electrically conducting non-Newtonian Power law fluid in a duct of circular cross-section has been considered. The geometry of the problem is shown in *Fig. 1*, where the cylindrical coordinate system (r,z) is located as shown. An external uniform magnetic field B0 is applied arbitrarily in the plane perpendicular to the z-axis.

The magnetic field exerts a restraining force on the conductor, which tends to impede its motion. This force is known to be proportional to its speed of motion and the magnetic field strength. The current flow in the conductor generates Joule's heat [8].

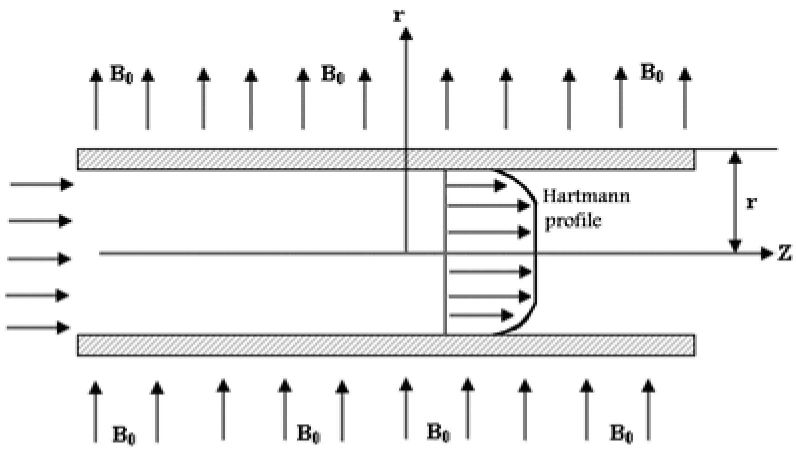

Fig. 1. Sketch of the problem.

The governing equations of the problem are:

Continuity equation

$$\nabla.\vec{V}=0. \tag{1}$$

Momentum equation

$$\rho\frac{D\vec{V}}{Dt}=\nabla.\left(\mu\nabla.\vec{V}\right)-\nabla P+\vec{F}_e. \tag{2}$$

Electromagnetic Lorentz force

$$\vec{F}_e=\vec{j}\times\vec{B_0}. \tag{3}$$

Energy equation

$$\rho C_P\frac{DT}{Dt}=\nabla.\left(K\nabla.T\right)+\Phi^{'}+\Phi^{''}. \tag{4}$$

Joule dissipation

$$\Phi^{''}=\sigma B_0^2 U^2. \tag{5}$$

Current density

$$\vec{j}=\sigma\vec{E}, \tag{6}$$

where $\vec{V}=v.\vec{e}_r+u.\vec{e}_z$ is the velocity vector of the fluid. Assuming a small magnetic Reynolds number (Re_m<<1), neglecting the induced magnetic field, and also assuming that there is no excess charge in the electrically conducting fluid guarantees that the induced electric field is negligible [3], [8]. An apparent viscosity is used for analogy, Non-Newtonian fluid (power law) to Newtonian fluid, given by

$$\mu=m\dot{\gamma}^{n-1};\ \dot{\gamma}=\frac{\partial u}{\partial r}. \tag{7}$$

The boundary conditions are given by

$$u(r=R,z)=0\ ,\quad \left(\frac{\partial u}{\partial r}\right)_{r=0}=0,$$
$$u(r,z=0)=u_0,\quad \left.\frac{\partial u}{\partial z}\right|_{z=1}=0. \tag{8}$$

The following two cases of the thermal boundary conditions are considered.

Case 1. A constant temperature at the wall where,

$$T(R,z)=T_W\ ,\ \left(\frac{\partial T}{\partial r}\right)_{r=0}=0,\ ,\quad T(r,z=0)=T_0. \tag{9}$$

Case 2. A constant heat flux at the wall, where

$$q^{''}=Cte,\quad \left(\frac{\partial T}{\partial r}\right)_{r=0}=0\quad ,T(r,z=0)=T_0. \tag{10}$$

Due to the axisymmetry of the problem, only one half of a cross-section of the duct (0≤R≤1/2 and 0≤L≤15) was considered.

Governing equations in the cylindrical coordinate system in two-dimensional forms have been written in the non-dimensional form, while the following non-dimensional variables and parameters were introduced [8]:

$$U=\frac{u}{u_0},\ V=\frac{v}{u_0},\ P=\frac{p-p_0}{\rho_0\, u_0^2},\ \bar{\mu}=\left(\frac{\partial U}{\partial R}\right)^{n-1},\ \bar{\mu}=\frac{\mu}{\mu_r},\ \mu_r=\frac{m u_0^{n-1}}{D^{n-1}},\ R=\frac{r}{D},\quad Z=\frac{z}{D},$$

$$\mathrm{Re}=\frac{\rho_0\, u_0 D}{\mu_r},\ \mathrm{Pr}=\frac{\mu_r.c_p}{k},\ \mathrm{Ha}^2=\frac{\sigma B_0^2 D^2}{\mu_r},$$

where

Case 1. $\theta=\frac{T-T_0}{T_w-T_0},\ \mathrm{Br}=\frac{\mu_r.u_0^2}{k\left(T_w-T_0\right)}$, and

Case 2. $\theta=\frac{T-T_0}{q'' D/k},\ \mathrm{Br}=\frac{\mu_r.u_m^2}{D q''}$. Thus, governing equations in dimensionless form are

Continuity equation

$$\frac{1}{R}\frac{\partial(VR)}{\partial R}+\frac{\partial U}{\partial Z}=0. \tag{11}$$

z- momentum equation

$$U\frac{\partial U}{\partial Z}+V\frac{\partial U}{\partial R}=-\frac{\partial P}{\partial Z}+\frac{1}{\mathrm{Re}}\left[\frac{1}{R}\frac{\partial}{\partial R}\left(\bar{\mu} R\frac{\partial U}{\partial R}\right)+\frac{\partial}{\partial Z}\left(\bar{\mu}\frac{\partial U}{\partial Z}\right)\right]-\frac{\mathrm{Ha}^2 U}{\mathrm{Re}}. \tag{12}$$

r- momentum equation

$$U\frac{\partial V}{\partial Z}+V\frac{\partial V}{\partial R}=-\frac{\partial P}{\partial R}+\frac{1}{\mathrm{Re}}\left[\frac{1}{R}\frac{\partial}{\partial R}\left(\bar{\mu} R\frac{\partial V}{\partial R}\right)+\frac{\partial}{\partial Z}\left(\bar{\mu}\frac{\partial V}{\partial Z}\right)-\bar{\mu}\frac{V}{R^2}\right]. \tag{13}$$

Energy equation

$$U\frac{\partial \theta}{\partial Z}+V\frac{\partial \theta}{\partial R}=\frac{1}{\mathrm{Re.Pr}}\left[\frac{1}{R}\frac{\partial}{\partial R}\left(R\frac{\partial \theta}{\partial R}\right)+\frac{\partial^2\theta}{\partial Z^2}\right]+\Phi_1+\Phi_2, \tag{14}$$

where Φ_1, viscous dissipation

$$\Phi_1=\frac{\mathrm{Br}.\bar{\mu}}{\mathrm{Re.Pr}}\left[2\left(\left(\frac{\partial U}{\partial Z}\right)^2+\left(\frac{\partial V}{\partial R}\right)^2+\left(\frac{V}{R}\right)^2\right)+\left(\frac{\partial V}{\partial Z}+\frac{\partial U}{\partial R}\right)^2\right], \tag{15}$$

where Φ_2 Joule dissipation

$$\Phi_2=\frac{\mathrm{Br.Ha}^2}{\mathrm{Re.Pr}}U^2. \tag{16}$$

Adding the continuity equation with the momentum and energy equation, the source term S has been introduced.

$$S=\frac{\partial}{\partial Z}\left(U\Phi-\Gamma_Z\frac{\partial\Phi}{\partial Z}\right)+\frac{1}{R}\frac{\partial}{\partial R}\left(RV\Phi-\Gamma_R\frac{\partial\Phi}{\partial R}\right),$$

$$S=(S_P\,R_P\,\Delta R\,\Delta Z)\Phi_P+S_C\,R_P\,\Delta R\,\Delta Z, \tag{17}$$

Where the source term, S, has been linearized in the usual manner and Φ is a general variable which can be replaced by U, V, or θ and Γ is the diffusion coefficient. Equations are discretized, using finite volume, where convection terms are discretized by the upwind method (*Fig. 2*).

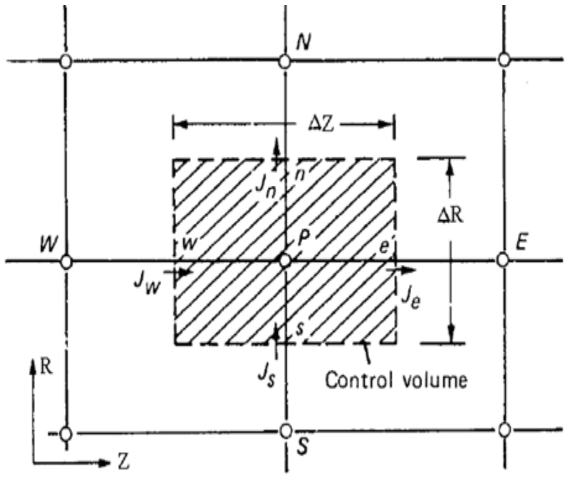

Fig. 2. Control volume for two-dimensional situations.

$$a_P\Phi_P=a_E\Phi_E+a_W\Phi_W+a_N\Phi_N+a_S\Phi_S+b, \tag{18}$$

where coefficients are:

$$a_P=a_E+a_W+a_N+a_S-S_P\,R_P\,\Delta R\,\Delta Z\quad b=S_C\,R_P\,\Delta R\,\Delta Z,$$

$$a_E=D_e+R_P\|-F_e,0\|,\;\; a_W=D_w+R_P\|F_w,0\|,\;\; a_N=D_n+\|-F_n,0\|,\;\; a_S=D_s+\|F_s,0\|,$$

$$D_s=\frac{\bar{\mu}_s\,R_s\,\Delta Z}{\mathrm{Re}\,\Delta R},\;\; D_n=\frac{\bar{\mu}_n\,R_n\,\Delta Z}{\mathrm{Re}\,\Delta R},\;\; D_e=\frac{\bar{\mu}_e\,R_P\,\Delta R}{\mathrm{Re}\,\Delta Z},\;\; D_w=\frac{\bar{\mu}_w\,R_P\,\Delta R}{\mathrm{Re}\,\Delta Z},$$

$$F_s=R_s\,V_s\,\Delta Z,\;\; F_n=R_n\,V_n\,\Delta Z,\;\; F_w=U_w\,\Delta R,\;\; F_e=U_e\,\Delta R.$$

A new operator ($\|A,B\|$) has been defined where ($\|A,B\|$) denotes the greater of A and B. The boundary conditions for the velocity are given:

$$U(R=0.5,Z)=0\,,\;\left(\frac{\partial U}{\partial R}\right)_{R=0}=0,\;\; U(R,Z=0)=1,\;\;\frac{\partial U}{\partial Z}\bigg|_{Z=L}=0. \tag{19}$$

The boundary conditions for the temperature are given:

Case 1. A constant temperature at the wall,

$$\theta(R=0.5,Z)=1\,,\;\left(\frac{\partial\theta}{\partial R}\right)_{r=0}=0,$$

$$\theta(r,z=0)=0. \tag{20}$$

Case 2. A constant heat flux at the wall,

$$\frac{\partial\theta}{\partial R}=1, \quad \left(\frac{\partial\theta}{\partial R}\right)_{R=0}=0, \qquad \textbf{(21)}$$
$$\theta(R,Z=0)=0.$$

The f.Re factor is defined as the product of the friction factor and the Reynolds number in the fully developed region and given by

$$f.Re=Re.D(-\frac{dp}{dz})/(0.5\rho u_0^2). \qquad \textbf{(22)}$$

The local Nusselt number for the two cases is given by

Case 1.

$$Nu_T=\left.\frac{\partial\theta}{\partial R}\right|_{R=0.5}, \qquad \textbf{(23)}$$

Case 2.

$$Nu_q=\frac{1}{\theta_W}, \qquad \textbf{(24)}$$

Where the average Nusselt number, Nu, for the two cases is given by

$$Nu_m=\frac{\bar{h}D}{k}=\frac{D}{k}\left(\frac{1}{L}\right)\int_0^L h\,dZ=\frac{1}{L}\int_0^L Nu_D\,dZ. \qquad \textbf{(25)}$$

The continuity, momentum, and energy equations are solved using a finite volume method and a simple algorithm in which convection terms are applied using the upwind scheme [9]. An iterative procedure algorithm has been used to solve the momentum continuity and energy equations.

The process is repeated until the criteria of convergence for the continuity equation, which is less than $10^{-6,}$ are satisfied. For the thermal boundary condition, the process is repeated until the criterion of convergence $(\theta^{new}-\theta^{old})/\theta^{new}\leq 10^{-7}$ is satisfied for temperature. The convergence is achieved by taking 30×2400 mesh points for both hydrodynamic and thermal parts.

3 | Results and Discussion

Table 1 and *Table 2* compare the values of the fluid velocity and (f.Re), in mid-line, with analytical results in Refs [10], for nonmagnetic. The comparison shows a very good agreement between those.

Table 1. Comparison values of the U velocity.

n	0.5	0.75	1	1.25	1.5
U_{max} numerical	1.663	1.855	1.99	2.107	2.195
U_{max} (analytical)	1.666	1.857	2	2.11	2.2

Table 2. Comparison value of f. Re.

n	0.5	0.75	1	1.5
f.Re	25.275	40.369	63.91	158.72
f.Re (analytical)	25.298	40.409	64	158.78

$$U_{max} = \frac{3n+1}{n+1}. \tag{26}$$

$$f\,Re = 8 \times 2^n \left(\frac{3n+1}{n}\right)^n.$$

Fig. 3 shows the variation of f.Re with Ha number (indicated power of magnetic field) for various values of n. *Fig. 3* shows that increasing the degree of shear of the fluid decreases the wall shear rate, where n becomes smaller, causing the viscosity to decrease even faster. The shear stress is the product of the shear rate and the viscosity; therefore, there will be a net increase in wall shear stress (i.e., f.Re). It is also found that increasing the Hartmann number increases the wall shear rate, causing an increase in wall shear stress (i.e., f.Re).

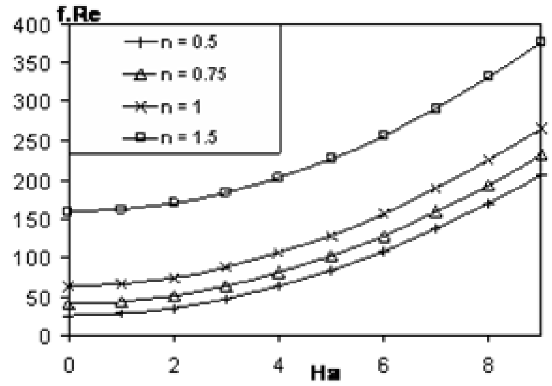

Fig. 3. Variation of f.Re with the Hartmann number.

Fig. 4 presents the variation of the maximum velocity U for the fully developed region. Due to the damping effect of the magnetic field, increasing the Hartmann number decreases the maximum velocity. *Fig. 4* also shows that increasing n increases the viscosity and wall shear stress, causing an increase in the maximum velocity.

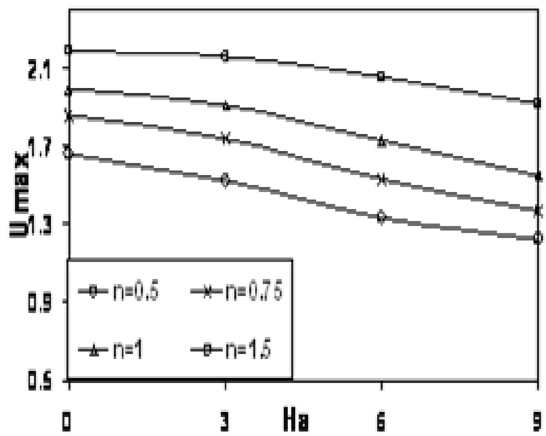

Fig. 4. Variation of U_{max} versus Ha.

The variation of the velocity U for the fully developed region of a circular cross-section with the radius R with respect to various values of Ha and n is shown in *Figs. 5-10*. Figs indicate that increasing Hartmann number decreases U for all values of n. Increasing the flow index n increases U for all values of the Hartmann number.

The velocity profile U becomes increasingly flattened with R for large values of Hartmann number (Ha=9) and shear thinning fluid (n=0.5), which is due to the damping effect of the magnetic field. *Fig. 5* indicates that for R<0.33, increasing the Hartmann number decreases velocity.

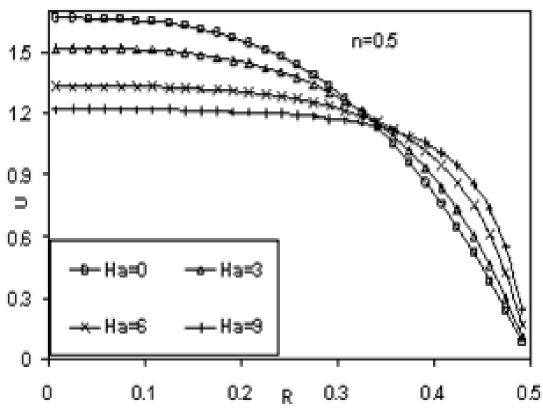

Fig. 5. Variation of U velocity versus R (n=0.5).

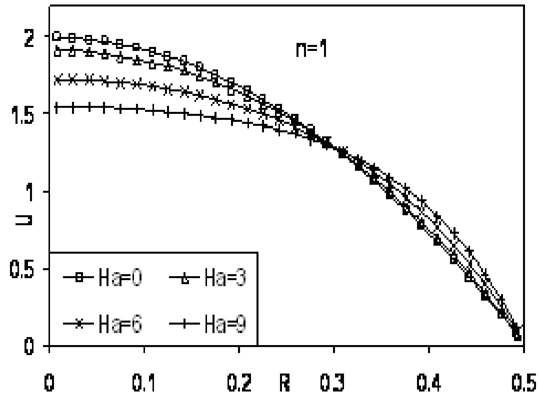

Fig. 6. Variation of U velocity versus R (n=1).

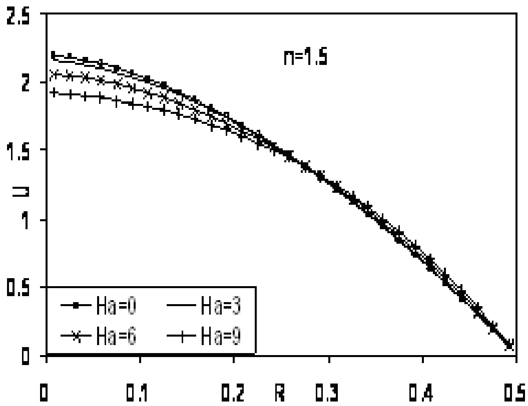

Fig. 7. Variation of U velocity versus R (n=1.5).

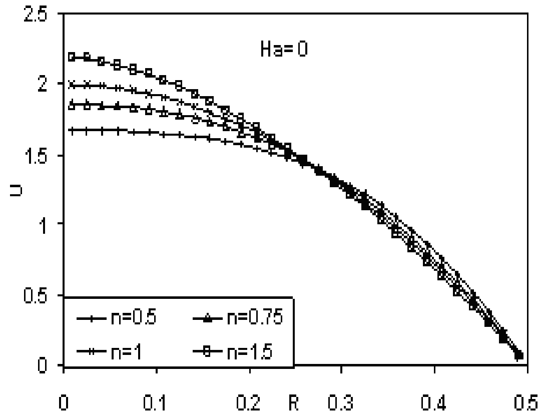

Fig. 8. Variation of U velocity versus R (Ha=0).

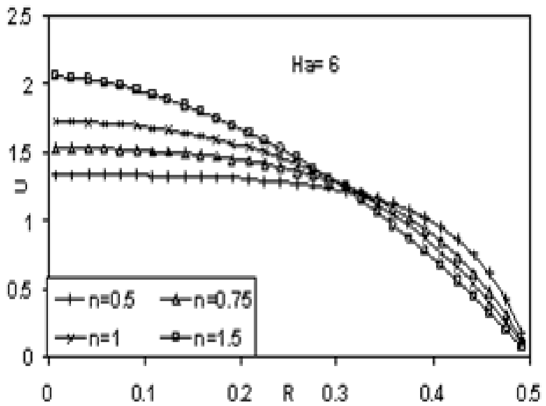

Fig. 9. Variation of U velocity versus R (Ha=6).

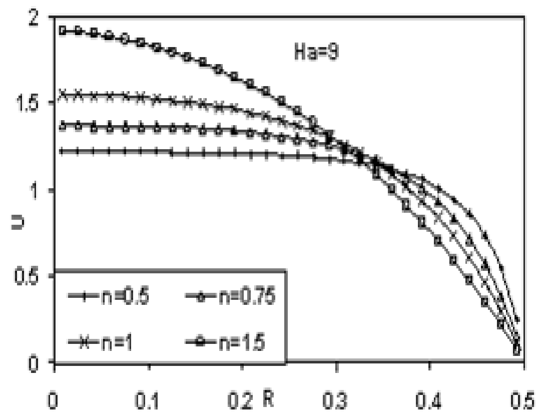

Fig. 10. Variation of U velocity versus R (Ha=9).

Figs. 11-16 show the variation of the average Nusselt number, Nu, for two defined cases with Hartmann number for various values of viscosity index, Pr, and Re, where the dissipation terms are assumed to be negligible for Br=0.

Figures show that increasing n decreases the average Nusselt number for all values of Hartmann number. However, increasing the Hartmann number increases Nu_m while increasing the Reynolds or Prandtl number increases Nu_m.

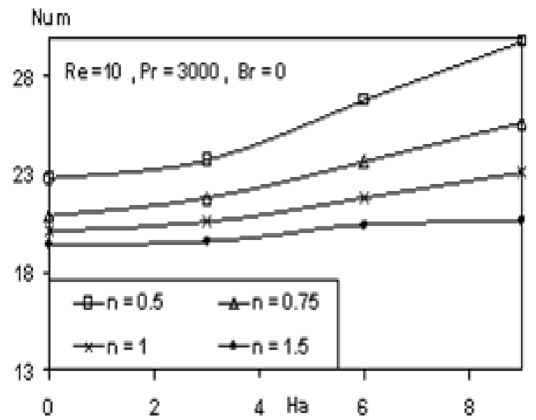

Fig. 11. Variation of Num versus Ha [case 1. Br=0, Pr=3000 & Re=10].

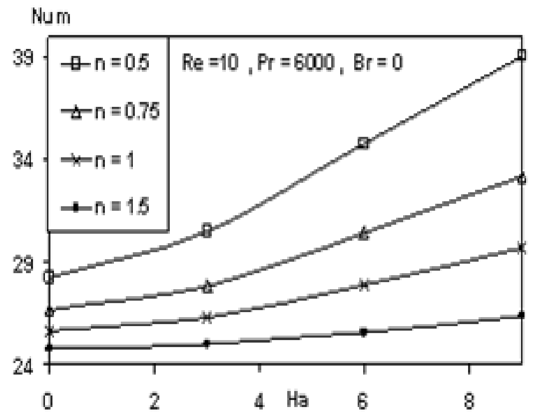

Fig. 12. Variation of num versus Ha [case 1. Br=0, Pr=6000 & Re=10].

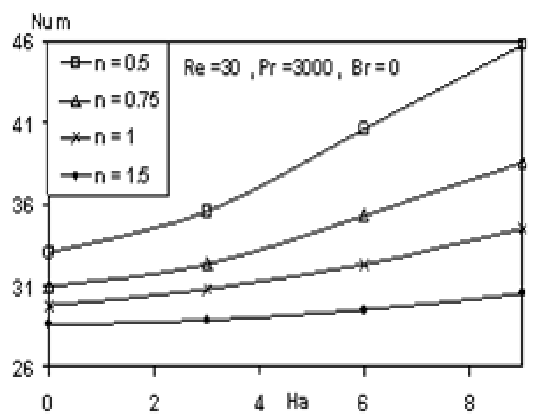

Fig. 13. Variation of num versus Ha [case 1. Br=0, Pr=3000 & Re=30].

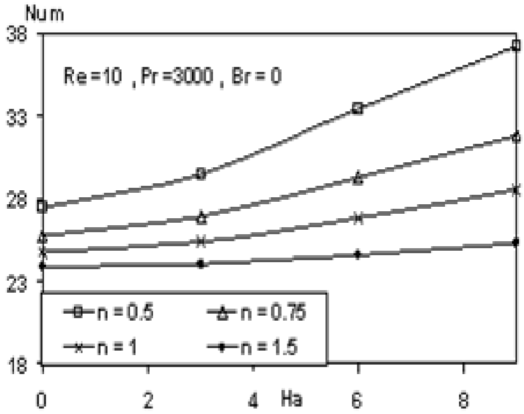

Fig. 14. Variation of num versus Ha [case 2. Br=0, Pr=3000 & Re=10].

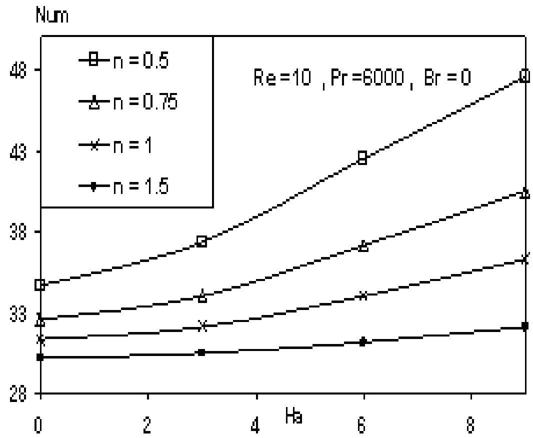

Fig. 15. Variation of num versus Ha [case 2. Br=0, Pr=6000 & Re=10].

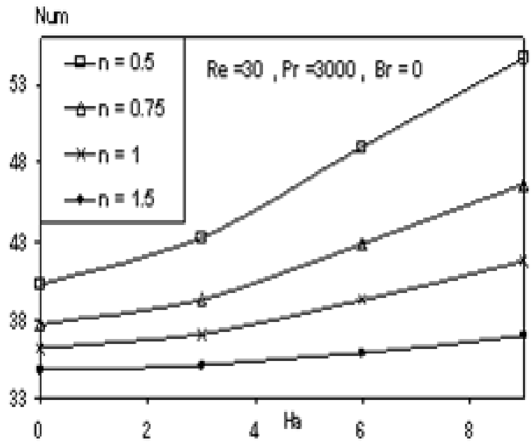

Fig. 16. Variation of num versus Ha [case 2. Br=0, Pr=3000, & Re=30].

The fact is that increasing the Hartman number or decreasing the viscosity index value decreases the wall shear rate, which causes an increase in thermal diffusion at the wall and follows an increase in Nusselt number.

Variation of the average Nusselt number, Nu_m, with Hartmann number and viscosity index, for *Case 1*, is shown in *Fig. 17* and *Fig. 18*, respectively. Figs show, for Br=0, increasing viscosity index and decreasing Nu_m, while increasing Hartmann number increases Nu_m. Variation of Nu_m versus Ha is more considerable for n<1. When Br=0.5, for small Hartmann (Ha<1), increasing n increases Nu_m, while for Ha>1, a reversed effect can be seen. When Br=1, increasing n increases Nu_m. Increasing Hartmann number decreases Nu_m up to n=0.65, while for n > 0.65, Nu_m increases gradually.

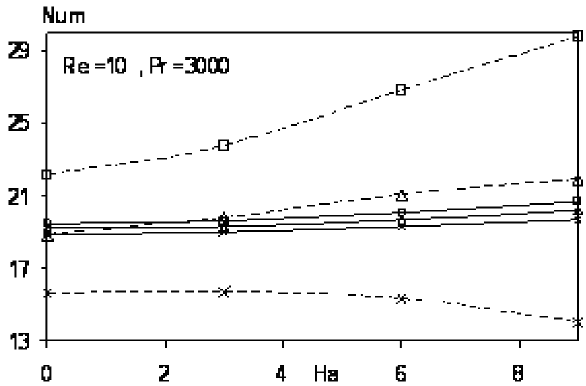

Fig. 17. Variation of num versus Ha [Pr=3000& Re=10]

Case 1. -- n=0.5, ——n=1.5, □Br=0, ΔBr=0.5, *Br=1.

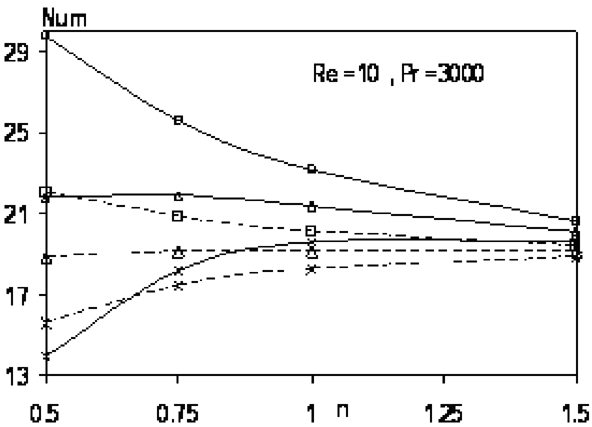

Fig. 18. Variation num versus n for Pr=3000, Re=10

Case 1. -- n=0.5, ——n=1.5, □Br=0, ΔBr=0.5, *Br=1.

The variation of the average Nusselt number, Nu_m, with Hartmann number and viscosity index for *Case 2* is shown in *Fig. 19* and *Fig. 20,* respectively. Figs show, for Br=0, increasing n decreases Nu_m while increasing Ha increases Nu_m. For Br = 0.5 and 1, increasing Ha decreases Nu_m while increasing n increases Nu_m. *Figs. 17-20* also indicate that increasing the Brinkman number decreases Nu_m for all values of Ha and n.

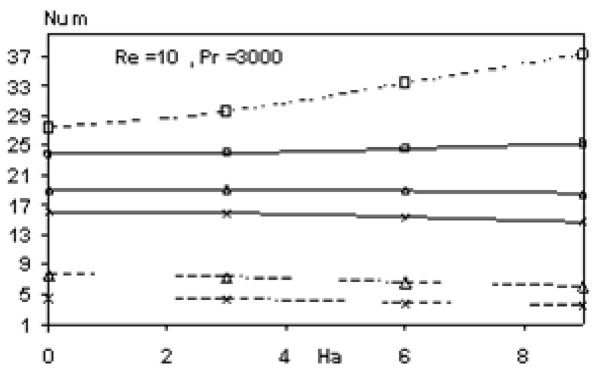

Fig. 19. Variation of num versus Ha for Pr=3000, Re=10,
Case 2. ---Ha=0, ——Ha=9, □Br=0, ΔBr=0.5, *Br=1.

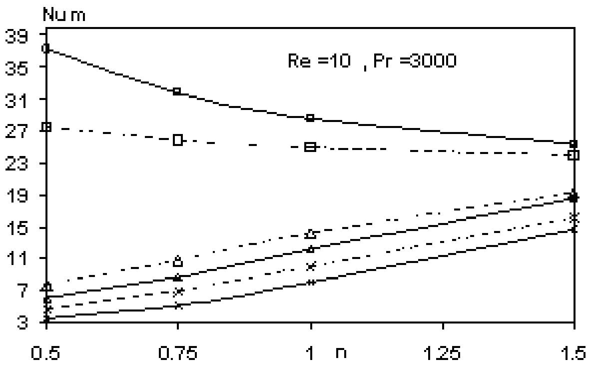

Fig. 20. Variation of num versus n for Pr=3000, Re=10, Case 2. – – –Ha=0, ——Ha=9, □Br=0, ∆Br=0.5, *Br=1.

Variation of the local Nusselt number for *Case 1* and *Case 2* versus the length of the pipe for different Br numbers is shown in *Figs. 21-23*. Figs present that increasing Br decreases the local Nusselt number. *Fig. 22* shows, for Br=1, at the end of the length of pipe (from 13.25 up to 15), there is a heat transfer from fluid to the wall.

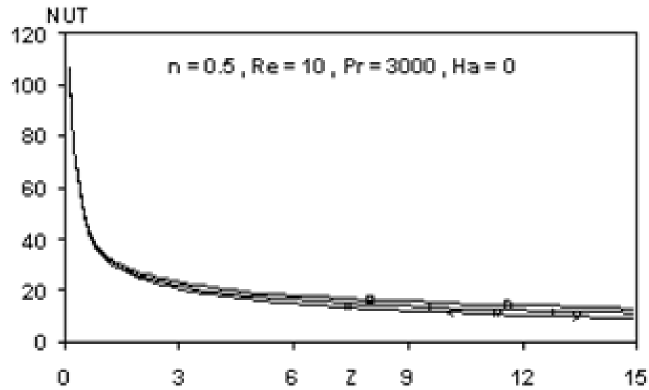

Fig. 21. Variation of local Nusselt versus length [Case 1] □Br=0,+ Br=0.5, *Br=1.

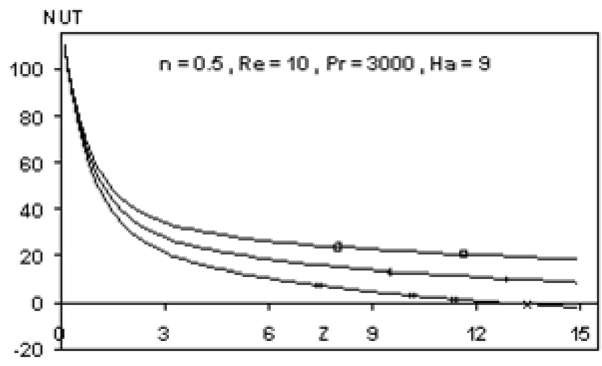

Fig. 22. Variation of local Nusselt versus length [Case 2] □Br=0,+ Br=0.5, *Br=1.

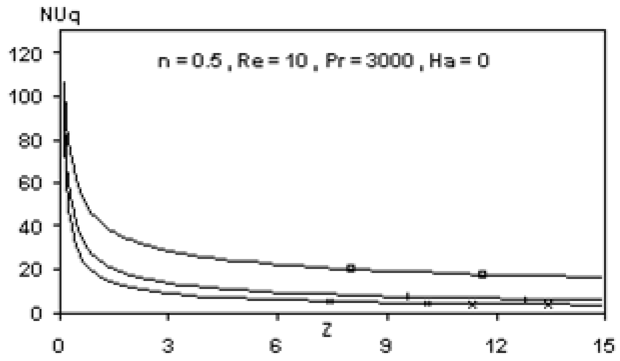

Fig. 23. Variation of local Nusselt versus length

[Case 1. □Br=0,+ Br=0.5, *Br=1].

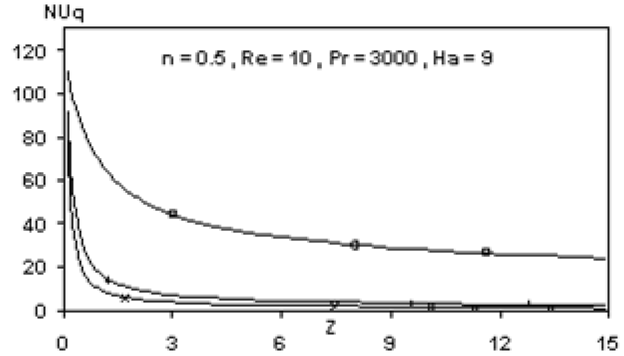

Fig. 24. Variation of local Nusselt versus length

[Case 2. □Br=0,+ Br=0.5, *Br=1].

The phenomenon can be explained by the fact that the heat generated by dissipation terms causes an increase in fluid temperature and results in a heat transfer from fluid to the pipe wall, consequently decreasing the Nusselt number.

4 | Conclusion

The steady laminar MHD flow of a viscous and incompressible conducting Non-Newtonian power law fluid in a circular duct was studied. The momentum and energy equations for two cases of thermal boundary conditions were solved numerically using the finite volume method. The effects of the magnetic field (Hartmann number) and the Non-Newtonian fluid characteristics (flow behavior index) on the flow and the heat transfer were discussed. Comparing the numerical results with analytical results for values of the maximum fluid velocity and friction factor for nonmagnetic reveals a good agreement.

The results show that the magnetic field has a damping effect on the flow for all values of the viscosity index, n. The increment in the Brinkman number decreases the value of the Nusselt number for all Hartmann numbers and viscosity index for two cases of thermal boundary conditions. Increasing the Hartmann number decreases maximum fluid velocity and increases the friction factor. Increasing the viscosity index increases maximum fluid velocity and friction factor.

Conflict of Interest

The authors declare that there is no conflict of interest regarding the publication of this article.

Data Availability

All data generated or analyzed during this study are included in this published article. No additional data are available.

Funding

This research did not receive any specific grant from funding agencies in the public, commercial, or not-for-profit sectors.

References

[1] Min, T., Choi, H. G., Yoo, J. Y., & Choi, H. (1997). Laminar convective heat transfer of a Bingham plastic in a circular pipe—II. Numerical approach hydrodynamically developing flow and simultaneously developing flow. *International journal of heat and mass transfer, 40*(15), 3689–3701. https://doi.org/10.1016/S0017-9310(97)00004-5

[2] Hossain, M. A. (1992). Viscous and Joule heating effects on MHD-free convection flow with variable plate temperature. *International journal of heat and mass transfer, 35*(12), 3485–3487. https://doi.org/10.1016/0017-9310(92)90234-J

[3] Jha, B. K. (2001). Natural convection in unsteady MHD Couette flow. *Heat and mass transfer, 37*(4), 329–331. https://doi.org/10.1007/PL00013295%0A%0A

[4] Sayed-Ahmed, M. E., & Attia, H. A. (2000). MHD flow and heat transfer in a rectangular duct with temperature dependent viscosity and Hall effect. *International communications in heat and mass transfer, 27*(8), 1177–1187. https://doi.org/10.1016/S0735-1933(00)00204-9

[5] Sayed-Ahmed, M. E., & Attia, H. A. (2005). The effect of Hall current on magnetohydrodynamic flow and heat transfer forBingham fluids in a rectangular duct. *Canadian journal of physics, 83*(6), 637–651. https://doi.org/10.1139/p05-006

[6] Attia, H. A. (2006). Hall effect on the flow of a dusty bingham fluid in a circular pipe. *Turkish journal of engineering & environmental sciences, 30*(1). 14-21. https://openurl.ebsco.com/EPDB%3Agcd%3A2%3A2736082/detailv2?sid=ebsco%3Aplink%3Ascholar&id=ebsco%3Agcd%3A21183349&crl=c&link_origin=scholar.google.com

[7] Sayed Ahmed, M. E. (2006). Numerical solution of power law fluids flow and heat transfer with a magnetic field in a rectangular duct. *International communications in heat and mass transfer, 33*(9), 1165–1176. https://doi.org/10.1016/j.icheatmasstransfer.2006.06.003

[8] Holman, J. P. (1996). *Heat transfer*. McGraw hill college. https://www.scribd.com/doc/52043947/Heat-Transfer-J-P-Holman

[9] Patankar, S. (2018). *Numerical heat transfer and fluid flow*. CRC press. https://doi.org/10.1201/9781482234213

[10] Skelland, A. H. P., & Flow, N. N. (1967). *Non-Newtonian Flow and Heat Transfer*. Wiley. https://books.google.nl/books/about/Non_Newtonian_Flow_and_Heat_Transfer.html?id=-07xAAAAMAAJ&redir_esc=y

Appendix

Nomenclature

B0: magnetic field.

Br: Brinkman number.

C_p: specific heat.

D: diameter of pipe.

E: electric field.

F: friction factor.

Fe: external magnetic force.

Ha: hartmann number.

J: current density.

K: thermal conductivity.

l: length of pipe.

m: consistency index of the model.

n: flow behavior index.

Num: average Nusselt number.

Nu_T, Nu_q: local Nusselt number.

P: pressure.

P_0: reference pressure.

Pr: prantl number.

q'': heat flux.

R: radius of pipe.

r,z: cylindrical coordinates.

Re: Reynolds number.

Re_m: magnetic Reynolds number.

T: temperature.

T_0: reference temperature.

Tw: temperature at the wall.

u: z component of the fluid velocity.

v: r component of the fluid velocity.

Greek symbols

ΔZ, ΔR: step size in Z and R coordinates.

σ : electric conductivity.

μ : apparent viscosity.

μ_r : reference viscosity of power law fluid.

$\bar{\mu}$: dimensionless apparent viscosity.

Φ' : viscous dissipation.

Φ'' : joule dissipation.

ρ_0 : reference density.

ρ : density.

θ : dimensionless temperature.

Φ : general variables.

$\dot{\gamma}$: shear rate.